Interaction of Yeast Rab Geranylgeranyl Transferase with Its Protein and Lipid Substrates†

Beatrice Dursina, Nicolas H. Thomä,‡ Vadim Sidorovitch, Anca Niculae, Andrei Iakovenko, Alexy Rak, Stefan Albert,§ Alice-Corina Ceacareanu,|| Ralf Kölling,⊥ Christian Herrmann, Roger S. Goody, and Kirill Alexandrov*

Max-Planck-Institute for Molecular Physiology, Otto-Hahn-Strasse 11, 44227 Dortmund, Germany

Received December 19, 2001; Revised Manuscript Received April 5, 2002

ABSTRACT: Small GTPases from the Rab/Ypt family regulate events of vesicular traffic in eukaryotic cells. For their activity, Rab proteins require a posttranslational modification that is conferred by Rab geranylgeranyltransferase (RabGGTase), which attaches geranylgeranyl moieties onto two cysteines of their C terminus. RabGGTase is present in both lower and higher eukaryotes in the form of heterodimers composed of α and β subunits. However, the α subunits of RabGGTases from lower eukaryotes, including *Saccharomyces cerevisiae* (yRabGGTase), are half the size of the corresponding subunit of the mammalian enzyme. This difference is due to the presence of additional immunoglobulin (Ig)-like and leucine rich (LRR) domains in the mammalian transferase. To understand the possible evolutionary implications and functional consequences of structural differences between RabGGTases of higher and lower eukaryotes, we have investigated the interactions of yeast RabGGTase with its lipid and protein substrate. We have demonstrated that geranylgeranyl pyrophosphate binds to the enzyme with an affinity of ca. 40 nM, while binding of farnesyl pyrophosphate is much weaker, with a K_d value of ca. 750 nM. This finding suggests that despite the structural difference, yRabGGTase selects its lipid substrate in a fashion similar to mammalian RabGGTase. However, unlike the mammalian enzyme, yRabGGTase binds prenylated and unprenylated Ypt1p:Mrs6p complexes with similar affinities (K_d ca. 200 nM). Moreover, in contrast to the mammalian enzyme, phosphoisoprenoids do not influence the affinity of Mrs6p for yRabGGTase. Using an in vitro prenylation assay, we have demonstrated that yRabGGTase can prenylate Rab proteins in complex with mammalian REP-1, thus indicating that neither the LRR nor the Ig-like domains, nor the recently discovered alternative pathway of catalytic complex assembly, are essential for the catalytic activity of RabGGTase. Despite the ability to function in concert with yRabGGTase in vitro, expression of mammalian REP-1 could not complement deletion of *MRS*6 gene in *S. cerevisiae* in vivo. The implications of these findings are discussed.

Posttranslational modification of proteins with farnesyl or geranylgeranyl groups is a widespread phenomenon in eukaryotic cells. These modifications are essential for protein function, modulating protein−protein or protein−lipid interaction. Many prenylated proteins, predominantly GTPases, play important roles in signal transduction pathways. This includes the subunits of heterotrimeric G proteins and many proteins of the Ras superfamily. Interest in protein prenylation has increased dramatically following the recognition of the importance of this modification for sustaining the transformed phenotype in many tumors (*1*, *2*).

During protein prenylation, either a farnesyl or a geranylgeranyl moiety is donated from soluble phosphoisoprenoids and attached to one or two C-terminal cysteine residues of the target protein via a thioether linkage. This type of reaction is catalyzed by three different protein prenyl transferases: protein farnesyltransferase (FTase), protein geranylgeranyl transferase-I (GGTase-I), and Rab geranylgeranyl transferase (RabGGTase of GGTase-II) (for a review, see ref *3*). The closely related FTase and GGTase-I transfer prenyl groups from prenyl diphosphates to proteins that contain a C-terminal CAAX motif (C is cysteine, A is usually an aliphatic amino acid, and X can be any of a number of different amino acids). The X residue of this motif largely determines the choice of isoprenoid.

† N.H.T was supported by an EMBO long-term fellowship. S.A was supported by a Max-Planck society pre-doctoral fellowship. This work was supported in part by a grant of the Deutsche Forschungs-Gemeinschaft AL 484/5-2 to K.A.

* To whom correspondence should be addressed. Tel.: +49 231 1332356. Fax: +49 231 1331651. E-mail: kirill.alexandrov@mpi-dortmund.mpg.de.

‡ Present address: Memorial Sloan-Kettering Cancer Center, Howard Hughes Medical Institute, 1275 New York Ave., New York, NY 10021.

§ Max-Planck-Institute of Biophysical Chemistry, Department of Molecular Genetics, D-37070, Goettingen, Germany.

|| Present address: University of Tennessee, Health Science Center College of Medicine, Department of Pharmacology, 874 Union Avenue, Memphis, TN, 38163.

⊥ Institute for Microbiology, Heinrich Heine Universität Düsseldorf, Universitätsstrabe 1, D-40225 Düsseldorf, Germany.

[1] Abbreviations: CHAPS, 3-[(3-cholamidopropyl)dimethylammonio]-1-propanesulfonate; Fpp, farnesyl pyrophosphate; FRET, fluorescence resonance energy transfer; GGpp, geranylgeranyl pyrophosphate; FTase, protein farnesyltransferase; GGTase-I, protein geranylgeranyltransferase type I; Mant, *N*-methylanthraniloyl; Mrs6p, yeast homologue of Rab escort protein; mFpp, mant-farnesyl pyrophosphate; mGpp, mant-geranyl pyrophosphate; REP, Rab escort protein; yRabGGTase, yeast Rab geranylgernyltransferase.

10.1021/bi016067w CCC: $22.00
Published on Web 05/04/2002

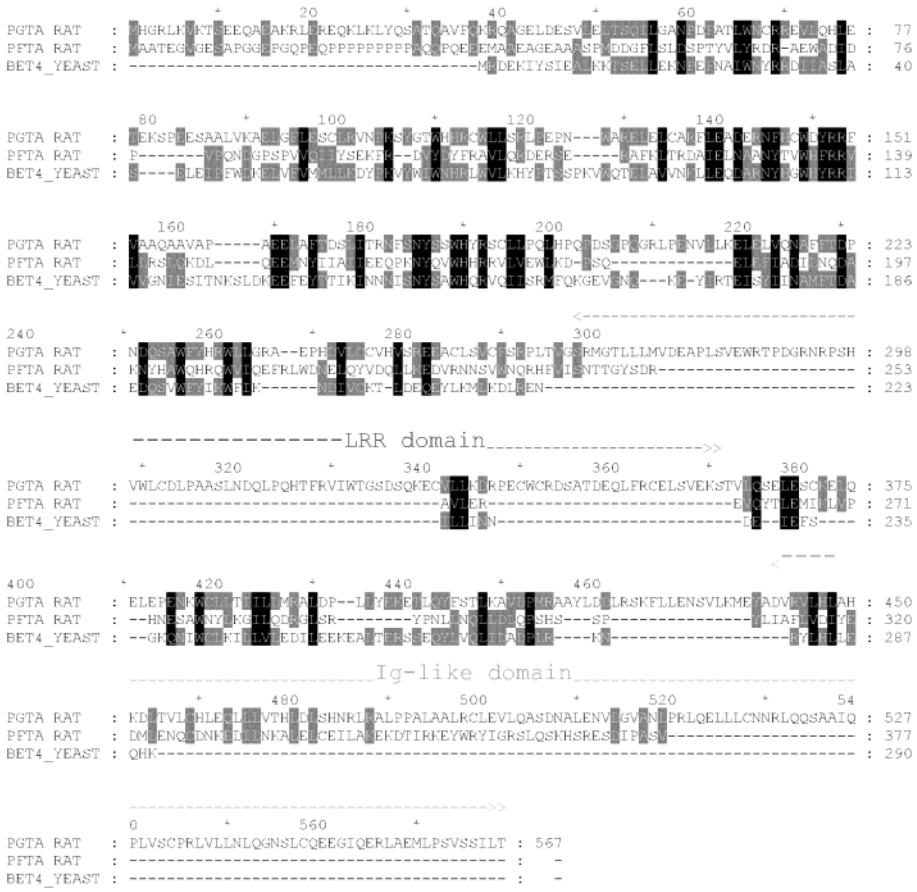

FIGURE 1: Sequence alignment of α subunits of mammalian RabGGTase (PGTA_RAT), yeast RabGGTase (BET4_YEAST), mammalian GGTase-I, and FTase (PFTA_RAT). The regions in mammalian RabGGTase corresponding with LRR and Ig domains are marked.

RabGGTase is quite different from other prenyl transferases, both functionally and structurally. Mammalian RabGGTase is a heterodimer composed of α and *β* subunits of 60 and 38 kDa, respectively, with the latter harboring a single prenyl binding site (*4*). The α subunit consists of a helical domain, followed by an immunoglobulin (Ig)-like fold and an additional leucine rich repeat (LRR). It has been suggested that the latter is involved in the interaction with Rab escort protein (REP) (Mrs6p or Mis4p in yeast nomenclature (*5*))—a multifunctional component that assists the prenylation reaction and delivers the product to the target membrane (*6*−*8*). Studies performed on mammalian RabGGTase have revealed two alternative pathways for the assembly of the catalytic complex. In the "classical" pathway, a newly synthesized Rab protein forms a stable complex with REP. RabGGTase, loaded with GGpp, recognizes the Rab:REP complex and covalently attaches the geranylgeranyl groups to two C-terminal cysteines of the Rab protein (*9*). Upon prenylation, the Rab:REP complex remains tightly associated with the transferase until binding of a new molecule of isoprenoid decreases its affinity for the prenylated complex (*10*). The prenylated complex dissociates from RabGGTase and delivers Rab protein to its target membrane (*7*, *11*). In the alternative pathway, RabGGTase and REP form a tight complex in the presence of the phosphoisoprenoid. This complex is catalytically competent and can recruit and prenylate Rab molecules (*12*). The kinetics of the actual prenylation reaction proceeding via either of the pathways appears to be identical, raising the question as to which of the two pathways is preferred in vivo. The discrimination between the two different pathways was proposed to depend on the concentration and distribution of the individual components in the cell (*12*).

Interestingly, the α subunit of yeast RabGGTase is noticeably smaller than its mammalian counterpart (35 and 65 kD, respectively) and has a higher sequence homology with the α subunits of GGTase-I and FTase than with mammalian RabGGTase. In particular, the regions comprising the LRR and Ig domains are missing in RabGGTase of yeast and invertebrates (Figure 1). It is currently not known whether the large structural differences between mammalian and yeast RabGGTase reflect differences in their reaction mechanisms. Moreover, there are no data available on the affinity of yeast RabGGTase for its isoprenoid or protein substrate. Studies on yeast FT and GGTase-I demonstrated that the affinities of the enzymes for lipid substrates were 10−100-fold weaker than of their mammalian counterparts (*13*−*16*).

In this study, we demonstrate that yeast RabGGTase follows the classical pathway of catalytic complex assembly and that it displays significantly lower affinity for its reaction product than its mammalian counterpart. We find that the LRR and Ig domains are dispensable for catalytic activity of RabGGTase. We propose that the alternative pathway of catalytic complex assembly was acquired late in the evolution of eukaryotes and might serve as an additional level of regulation of the geranylgeranylation pathway.

MATERIALS AND METHODS

Preparation of Fluorescent Analogues of GGpp and Fpp. The synthesis of fluorescently labeled analogues of GGpp and Fpp was performed as described (*17*).

Expression and Purification of Mammalian RabGGTase, REP-1, Rab7, Ypt7p, and Ypt1p. Expression and purification of wild-type Rab7, Ypt7p, Ypt1p, RabGGTase, and REP-1 were performed as described (*18*−*21*).

Cloning, Expression, and Purification of Saccharomyces cerevisiae RabGGTase in Escherichia coli. We initially attempted to use the translationally coupled bicistronic construct pDJW-1-244/7 described earlier (*22*). We found that following IPTG induction, only one protein of ca. 34 kDa was induced. The protein was insoluble, and using Edman degradation sequencing, we identified it as Bet4p. In an attempt to obtain the active heterodimer of Bet2p (α subunit) and Bet4p (β subunit), we inserted the entire BET2/BET4 assembly into the pET-22b vector using the NdeI and blunted KpnI sites cloned into the NdeI and blunted BamHI site. The resulting construct was designated pET22-BET4-BET2 and was used for optimization of the ribosomal binding site yielding constructs pET22-BET4-BET2-1 and pET22-BET4-BET2-2. Again, the only protein expressed was Bet4. To express Bet2p, we amplified its open reading frame by polymerase chain reaction (PCR) using genomic yeast DNA as a template with primers containing an NdeI site in front of the start codon and a SalI restriction site after the termination codon. The resulting product was digested with NdeI and SalI and ligated into the pGATEV vector precut with NdeI and XhoI enzymes (*19*). The resulting construct was designated pGATEV-BET2. For protein production, *E. coli* BL21(DE3) cells were cotransformed with pGATEV-BET2/pET22-BET4-BET2 and selected on LB plates with ampicillin (125 μg/mL) and kanamycin (35 μg/mL). Cells were grown on LB medium containing ampicillin (125 μg/mL) and kanamycin (35 μg/mL) at 37 °C, induced when the OD_{600} was close to 0.9, and then incubated at 20 °C for 12 h. After cell growth, cells were pelleted (5000 g, 15 min at 4 °C), resuspended in lysis buffer (50 mM Na_2HPO_4, pH 8.0, 0.3 M NaCl, 2 mM β-mercaptoethanol (BME), and 1 mM PMSF), and lysed by passing twice through a fluidizer (Microfluidics). The resulting homogenate was clarified by centrifugation (30 000*g*, 1 h at 4 °C) and filtered through a 0.45 μm nitrocellulose filter (Schleiher and Schuell). The filtrate was loaded onto a 5 mL Hi-Trap Ni-NTA column (Pharmacia) preequilibrated with the lysis buffer. The column was washed extensively with lysis buffer containing 5 mM imidazole, and the bound protein was eluted with a linear 5−200 mM imidazole gradient in 30 column volumes. Eluates were analyzed by sodium dodecyl sulfate polyacrylamide gel electrophoresis (SDS−PAGE) followed by Coomassie blue staining. Fractions containing yeast RabGGTase were pooled, TEV protease was added at a 1:40 molar ratio, and the sample was dialyzed against 25 mM Na_2HPO_4, pH 8.0, 1 mM ethylenediaminetetraacetic acid (EDTA), and 2 mM BME for 12 h at 4 °C. The progression of the cleavage reaction was monitored by SDS−PAGE, and typically, at the end of the incubation, over 95% of protein was cleaved. To remove the polyhistidine tags, uncleaved protein, TEV protease, and impurities, $MgCl_2$ was added to the sample to 2 mM and imidazole to 25 mM, and the protein was passed twice over a 5 mL Hi-Trap Ni-NTA column (Pharmacia). The flow-through of the column, which contained yeast RabGGTase, was dialyzed against 25 mM *N*-(2-hydroxyethyl)piperazine-*N*′-ethanesulfonic acid (HEPES), pH 7.2, 25 mM NaCl, and 5 mM dithiothreitol (DTT), concentrated using Centriprep 30 (Amicon), and stored in multiple aliquots at −80 °C. For purification of the enzyme with an intact GST tag, the eluate from the Ni-NTA column was diluted 10-fold with water and loaded onto a 10 mL Poros HQ50 column equilibrated with 5 mM Na_2HPO_4, 50 mM NaCl, and 2 mM BME. The column was developed with a 50−300 mM linear gradient of NaCl in 25 column volumes. Fractions containing pure GST-yeast RabGGTase were collected, dialyzed against 25 mM HEPES, pH 7.2, 25 mM NaCl, and 5 mM DTT, concentrated to ca. 10 mg/mL, and stored at −80 °C.

Expression and Purification of Mrs6p. The open reading frame of MRS6 was amplified by PCR using genomic yeast DNA as a template with specific primers containing *Nde*I upstream of the start codon and *BamH*I site immediately downstream of the stop codon. The PCR product was digested with *Nde*I and *BamH*I and inserted into pET30 precut with the same enzymes. The resulting plasmid was designated pET30-MRS6. For protein production, *E. coli* BL21-(DE3) cells were transformed with pET30-MRS6 and selected on LB plates with kanamycin (35 μg/mL). Cells were grown in LB medium containing kanamycin (35 μg/mL) at 37 °C, induced when the OD_{600} was close to 0.7, and then incubated at 20 °C for 12 h. Cells were pelleted by centrifugation and stored at −80 °C. For protein purification, the cell pellet was resuspended in 20 mM $NaHPO_4$, pH 8.0, 50 mM NaCl, 25 mM BME, and 1 mM PMSF and disrupted by passing twice through a fluidizer. The lysate was cleared by centrifugation, and $(NH_4)_2SO_4$ was added to a final concentration of 30% (w/v). The precipitated protein was separated by centrifugation, and another portion of $(NH_4)_2SO_4$ was added to the supernatant to give a final concentration of 55%. The precipitated protein was removed by centrifugation and resuspended in 20 mM $NaHPO_4$, pH 8.0, 50 mM NaCl, and 25 mM BME. The sample was dialyzed overnight against the same buffer and loaded onto a 20 mL POROS HQ column equilibrated with 20 mM $NaHPO_4$, pH 8.0, 50 mM NaCl, and 5 mM BME. The column was developed with a linear 100−600 mM NaCl gradient in 20 column volumes. Mrs6p eluted at ca. 300 mM NaCl. Fractions containing Mrs6p were concentrated to 10 mL and loaded onto a Superdex 200 26/60 column equilibrated with 25 mM HEPES, pH 7.2, 25 mM NaCl, and 10 mM dithioerythritol (DTE). Fractions containing Mrs6p were pooled, concentrated to 10 mg/mL, and snap-frozen in liquid nitrogen. The SDS−PAGE gel of proteins used in this investigation is shown in Figure 2b.

In Vitro Prenylation and Purification of Ypt1pGG:Mrs6p Complex. Protein complex formation and in vitro prenylation were performed in 10 mL of 40 mM HEPES/NaOH, pH 7.2, 50 mM NaCl, 5 mM DTE, 3 mM $MgCl_2$, 10 μM GDP, and 0.3% CHAPS. A 10 mL mixture contained 0.20 μmol of Mrs6p, 0.3 μmol of Ypt1p, 0.3 μmol of GST-yeast RabGGTase, and 2 μmol of GGpp. The sample was incubated at 27 °C for 5 min, adjusted to 2% CHAPS, and applied to a 3 mL Glutathion-Sepharose (Pharmacia) column equilibrated with reaction buffer containing 2% CHAPS. The flow-

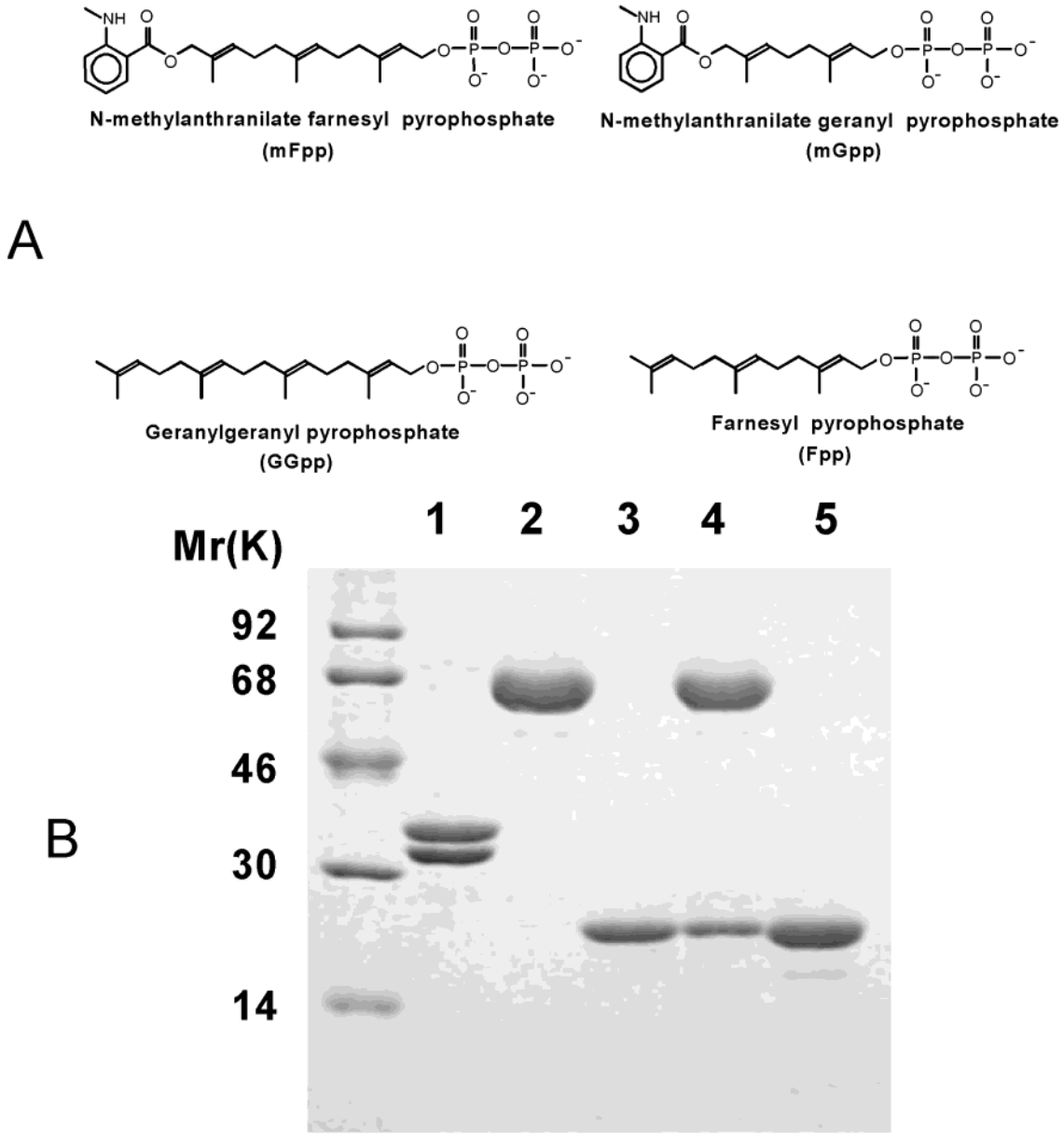

FIGURE 2: Phosphoisoprenoids used in this investigation. (A) Proteins used in this work (1) yRabGGTase, (2) Mrs6p, (3) wild-type Ypt1p, (4) prenylated Ypt1p:Mrs6p complex, and (5) wild-type Ypt7p protein. Approximately 1 μg of each protein was resolved on the 15% SDS−PAGE gel and subsequently stained with Coomassie blue. Mrs6p is well-stained with Coomassie and therefore appears to be more abundant than it actually is (B).

through was collected and concentrated using a Centriprep 10 (Amicon) to a final volume of 7 mL. The sample was centrifuged in a benchtop centrifuge for 5 min at 4 °C and loaded onto a 16/60 Superdex 200 (Pharmacia) gel filtration column equilibrated in 40 mM HEPES/NAOH, pH 7.2, 50 mM NaCl, 5 mM DTE, 3 mM $MgCl_2$, and 100 μM GDP. The flow rate was 2 mL/min, and fractions of 4 mL were collected and analyzed by SDS−PAGE. Fractions containing the Ypt1pGG:Mrs6p binary complex were pooled, concentrated, and stored in multiple aliquots at −80 °C. The homogeneity of double prenylation was confirmed by MALDI-TOF and high-performance liquid chromatography (HPLC) analysis as described (*19*, *23*).

In Vitro Prenylation Assay. In vitro prenylation reactions were performed essentially as described in ref *24*. Briefly, in a typical reaction volume of 50 μL, 40 pmol of pairwise combinations of Mrs6p or REP-1 with Ypt7p or Rab7 were mixed with 3 pmol of mammalian or yeast RabGGTase. The reaction was initiated by the addition of 100 pmol of tritiated geranylgeranyl pyrophosphate with a specific radioactivity in the range of 4000 cpm/pmol. All reactions were carried out at 30 °C in 25 mM HEPES, pH 7.2, 40 mM NaCl, 2 mM $MgCl_2$, 2 mM DTE, and 2 mM NP40. After 30 min, the reaction was quenched by addition of 2 mL of 10% HCl (37%) in 90% ethanol (v/v). The solution was incubated for 30 min at room temperature and subsequently filtered through glass fiber filters (Whatman). The filters were washed twice with 96% ethanol, immersed in scintillation liquid, and counted for [^{3}H].

Isothermal Titration Calorimetry and Fitting of the Data. Yeast RabGGTase/Mrs6p interactions were monitored using an isothermal titration calorimeter (MCS-ITC, MicroCal, Inc.) as described elsewhere (*25*). The data were analyzed using the manufacturer's software yielding the stoi-

chiometry (N), the binary equilibrium association constant (K_a), and the enthalpy of binding (ΔH_0). ΔH_0 was assumed to be independent of primary ligand concentration. From the relationship $\Delta G_0 = -RT \ln K_a$ and the Gibbs−Helmholtz equation, the free energy (G_0) and entropy of association (S_0) were calculated.

Labeling of Ypt1p Protein with the Dansyl Group. Labeling of Ypt1pp was performed essentially as described (*18*). Briefly, 50 nmol of wild-type Ypt1p was incubated with 1μmol of 1,5-IAEDANS (Molecular Probes) in 300 μL of 100 mM Tris, pH 8.0, 1 mM $MgCL_2$, and 100 μM GDP for 2 h at 4 °C. After the incubation period, the protein was passed through two 3 mL Sephadex G-25 (Pharmacia) spin columns preequilibrated with 20 mM HEPES, pH 7.2, 10 mM NaCI, 1 mM $MgCl_2$, 100 μM GDP, and 2 mM DTE. Labeled protein was stored at −80 °C.

Fluorescent Measurements. Fluorescence spectra and long time base fluorescence measurements were performed with an Aminco SLM 8100 spectrophotometer (Aminco). Reactions were carried out at 25 °C in 25 mM HEPES, pH 7.2, 40 mM NaCI, 2 mM $MgCI_2$, 2 mM DTE, and 100 μM GDP. Stopped flow experiments were performed in a SF61 apparatus (High-Tech Scientific).

Analysis of Titrations of N-Methylanthraniloyl (Mant)-Labeled Phosphoisoprenoid vs Increasing Concentrations of RabGGTase. The analysis was performed essentially as described (*26*). Briefly, titrations were fitted to the explicit solution of the quadratic equation describing the $E + S \leftrightarrows ES$ binding equilibrium, where K_d is defined as $K_d = [E] \times [S]/[ES]$. For mFpp:yRabGGTase titrations, the concentration of the mant-labeled phosphoisoprenoid was fixed [S_0], and increasing concentrations of yeast RabGGTase [E_0] were added. [E_0] and [S_0] refer to the total concentrations, free plus bound, of enzyme and substrate, respectively, in the cuvette. Under these conditions, the fluorescence is described by

$$F = F_{min} + (F_{max} - F_{min}) \times (([E_0] + [L_0] + K_d)/2 - ([E_0] + [L_0] + K_d)^2/4 - [E_0] \times [L_0])^{1/2}/[L_0]$$

where F represents the measured fluorescence intensity, while F_{min} and F_{max}, respectively, refer to the minimal and maximal fluorescence intensities observable. For mGpp:yRabGGTase titrations, the concentration of enzyme was fixed and increasing concentrations of mGpp were added. The fit was performed as described above.

Analysis of Competitive Titrations. The analysis was performed essentially as described (*26*). Briefly, the competitive titrations were performed by titrating a mixture of mant-labeled and unlabeled phosphoisoprenoid against increasing concentrations of yeast RabGGTase.

This data analysis was done via least-squares fitting using the program Scientist (MicroMath Scientific Software), where the following binding equilibria were used (*26*).

$$E + \text{mant} - S \leftrightarrows E - \text{mant} - S \quad K_{d-\text{mant}}$$

$$E + \text{unlabeled} - S \leftrightarrows E - \text{unlabeled} - S \quad K_{d-\text{unlabeled}}$$

During least-squares fitting, K_{d-mant}, which was determined in an independent experiment, was held constant, and $K_{d-unlabeled}$ was allowed to vary. $K_{d-unlabeled}$ obtained by this approach represents an absolute K_d and not a K_d value relative to the K_{d-mant}.

Global Fitting Procedures for Stopped Flow Experiments. The analysis was performed essentially as described (*26*). Briefly, data collection for the global fit procedures was carried out in two stages. First, stopped flow traces were collected using different concentrations of mant-labeled phosphoisoprenoid mixed with constant concentrations of yeast RabGGTase. Global fitting of data from several experiments was used to determine the rate constants and fluorescence yields for the binding of fluorescent isoprenoid to RabGGTase. The parameters were determined using a numerical integration procedure of a set of differential equations describing the binding model

$$E + A \underset{k_{-1}}{\overset{k_{+1}}{\leftrightarrows}} EA_1 \underset{k_{-2}}{\overset{k_{+2}}{\leftrightarrows}} EA_2$$

$$d[E]/dt = [EA_1] \times k_{-1} - [A] \times [E] \times k_{+1}$$

$$d[A]/dt = [EA_1] \times k_{-1} - [A] \times [E] \times k_{+1}$$

$$d[EA_1]/dt = [E] \times [A] \times k_{+1} + k_{-2} \times [EA_2] - [EA_1] \times (k_{+2} + k_{-1})$$

$$d[EA_2]/dt = [EA_1] \times k_{+2} - k_{-2} \times [EA_2]$$

(differential equation system 1)

Fluorescence (F) was defined as $F = \text{offset} + \text{yield1} \times [EA_1] + \text{yield2} \times [EA_2]$, assuming that both species could give rise to fluorescence changes.

To obtain the data for unlabeled isoprenoids, a mixture of mant−phosphoisoprenoid and varying concentrations of unlabeled isoprenoid were mixed with a constant concentration of yeast RabGGTase using constant instrument settings. The previously determined fluorescent yields and rate constants for the fluorescently labeled phosphoisoprenoid were used in the analysis of the competitive experiments. Knowing the binding parameters and fluorescent yields of the fluorescently labeled substrate, it was possible to extract the binding parameters of the nonlabeled substrate. The fluorescent yields could be inferred from the first stage to the second, since the photomultiplier voltage of the stopped flow instrument remained constant. The following differential equations were used in the analysis

$$E + B \underset{k_{-3}}{\overset{k_3}{\leftrightarrows}} EB_1 \underset{k_{-4}}{\overset{k_4}{\leftrightarrows}} EB_2$$

describing the binding of the unlabeled substrate, for example, GGpp or Fpp,

$$d[E]/dt = [EB_3] \times k_{-3} - [B] \times [E] \times k_{+3}$$

$$d[B]/dt = [EB_1] \times k_{-3} - [B] \times [E] \times k_{+3}$$

$$dE[B_1]/dt = [E] \times [B] \times k_{+3} + k_{-4} \times [EB_2] - [EB_1] \times (k_{+4} + k_{-3})$$

$$dE[B_2]/dt = [EB_1] \times k_{+4} - k_{-4} \times [EB_2]$$

(differential equation system 2)

and the differential equation system 1, as outlined above.

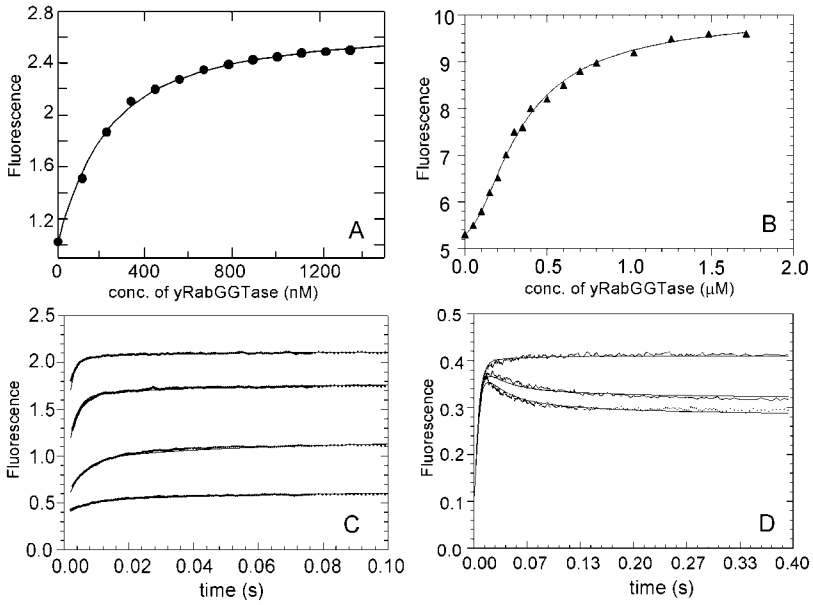

FIGURE 3: Fluorescence titration of mFpp (200nM) vs increasing concentrations of yRabGGTase. The fitted curve corresponds to a K_d of 200 ± 16 nM (A). Competitive titration in which 150 nM of mFpp was mixed with 150 nM of GGpp. The mixture was titrated with increasing concentrations of yRabGGTase. The K_d determined form the fit for GGpp was 14 ± 2 nM (B). Stopped flow traces of yRabGGTase rapidly mixed with mFpp (C) or a mixture of mFpp and GGpp (D). The signal was based on fluorescence resonance energy transfer, exciting at 289 nm, while data collection was performed with a 390 nm cutoff filter. In panel C, 50 nM yRabGGTase was mixed with increasing concentrations of mFpp (100, 200, 400, and 700 nM). The global fit obtained resulted in the following rate constants: $k_{+1} = 0.2$ s^{-1} nM^{-1}, $k_{-1} = 128$ s^{-1}, $k_{+2} = 11$ s^{-1}, and $k_{-2} = 16$ s^{-1}. In panel D, 100 nM of RabGGTase was mixed with 100 nM of mFpp and increasing concentrations of GGpp (200, 400, and 600 nM). The fit corresponds to $k_{+1} = 0.28$ s^{-1} nM^{-1}, $k_{-1} = 14$ s^{-1}, $k_{+2} = 3.7$ s^{-1}, and $k_{-2} = 6$ s^{-1}.

Because GGpp and Fpp do not fluoresce, they do not contribute to the signal. The fluorescence (*F*) is therefore only determined by mant-labeled compounds described by eq 1: F = offset + yield1 × [EA_1] + yield2 × [EA_2] assuming that both species, EA_1 and EA_2, could give rise to fluorescence changes. The rate constants obtained by this approach represent absolute rate constants and not rate constants relative to those of the unlabeled isoprenoid.

S. cerevisiae Complementation Studies. The yeast *S. cerevisiae* strain Y21667 (MATa/α, *his3*Δ*1*/*his3*Δ*1*, *leu2*Δ*0*/*leu2*Δ*0*, *lys2*Δ*0*/*LYS2*, *MET15*/*met15*Δ*0*, *ura3*Δ*0*/*ura3*Δ*0*, *MRS6*::*kanMX4*/*MRS6*) was purchased from EUROSCARF (Germany). The plasmid pYX212 was from the Research and Development (Abingdon, U.K.). The plasmid pYX212/REP-1 will be described elsewhere (Sidorovitch et al., submitted for publication).

Yeast cells were transformed with plasmid DNA using the lithium acetate/ss-DNA/PEG procedure of (*27*) and selected on SD-Ura plate. Single colonies of strains Y21667 and Y21667/pYX212/REP-1 were inoculated into 3 mL of YPAD {Sherman, 1991 480/id} and SD/CAS/Trp (0.67% Yeast Nitrogen Base with ammonium sulfate, 1% casamino acids (Difco), 2% D-(+)-glucose, L-tryptophan, and 20 mg/L) media, respectively. Cultures were incubated at 26 °C for 24 h, washed with 5 mL of sterile water, and resuspended in 3 mL of liquid sporulation medium (1% potassium acetate; 0.005% zinc acetate; L-histidine-HCl, 10 mg/L; L-leucine, 15 mg/L; L-lysine-HCl, 15 mg/L; and L-methionine, 10 mg/L). For the strain Y21667, uracil was added to the medium to reach a final concentration of 10 mg/L. Sporulation cultures were incubated at 26 °C for 3 days before dissection.

RESULTS

In this study, we set out to investigate the interaction of yeast RabGGTase (yRabGGTase) with its protein and lipid substrates and to establish whether the significant structural differences between mammalian and yeast enzyme are associated with differences in the reaction mechanisms.

Interaction of Yeast RabGGTase with GGpp. To analyze the interaction of yRabGGTase with phosphoioprenoids, we employed a fluorescence assay that uses two fluorescent mant-labeled isoprenoid derivatives, mGpp and mFpp, that can act as substrates of mammalian RabGGTase in vitro (Figure 2a) (*17*, *26*). On addition of yRabGGTase to a solution of mFpp, a fluorescence increase of more than 40% was observed when the mant group was excited at 333 nm and data was collected at 430 nm (data not shown). Determination of the affinity of RabGGTase for GGpp was performed in two stages. First, the affinity of RabGGTase for mFpp was determined via direct titration of RabGGTase vs fluorescent isoprenoid. Next, a competitive titration of RabGGTase against a mixture of mFpp and GGpp was carried out to allow calculation of the affinity of RabGGTase for GGpp. Titration of mFpp with increasing concentration of RabGGTase resulted in a saturable increase of fluorescence that could be fitted to K_d values of 200 ± 16 nM (Figure 3a). Titrations were subsequently carried out under competitive conditions to determine the K_d values for the interaction of RabGGTase with GGpp and Fpp. We mixed equal amounts of mFpp and GGpp, and the resulting solution was titrated with increasing concentrations of yRabGGTase. As can be seen in Figure 3b, there is an initial "lag" in the fluorescence increase, indicating that GGpp binds more strongly than mFpp to the transferase. The data were fitted

Scheme 1: Nomenclature of Kinetic Rate Constants Used in This Study[a]

Two-step binding:

$$\text{RabGGTase + Xpp} \underset{k_{-1}}{\overset{k_{on}}{\rightleftharpoons}} \text{RabGGTase-Xpp} \underset{k_{-2}}{\overset{k_{+2}}{\rightleftharpoons}} \text{RabGGTase-Xpp}^{*}$$

[a] The phosphoisoprenoid substrate is referred to as Xpp.

numerically using the program Scientist and lead to a K_d value of 14 ± 2 nM for the GGpp:yRabGGTase interaction (Figure 3b).

Transient Kinetics of yRabGGTase:GGpp Interaction. Having obtained the equilibrium parameters for GGpp and mFpp binding, we wanted to characterize the rate constants involved in this process. Stopped flow experiments were carried out using 50 nM yRabGGTase and increasing concentrations of mFpp. Primary data analysis indicated that mFpp binding to RabGGTase is a multistep process since the association transients were not simple exponential curves when mFpp was in large excess. The data were fitted using numerical integration of a set of differential equations describing a two step binding mechanism (see Materials and Methods and ref *26*). This procedure resulted in an excellent fit to the observed data (Figure 3c). On the basis of these fits, fluorescent yields for each species in combination with the following rate constants were determined, $k_{+1} = 0.2\ s^{-1}\ nM^{-1}$, $k_{-1} = 128\ s^{-1}$, $k_{+2} = 11\ s^{-1}$, and $k_{-2} = 16\ s^{-1}$ (Scheme 1). On the basis of these four rate constants, we could calculate a K_d value of 380 nM, which is in reasonable agreement with the previously determined K_d of 200 nM.

The kinetic parameters for GGpp binding were obtained from a competition experiment where 100 nM yRabGGTase was mixed with 100 nM of mFpp and increasing concentrations of GGpp. An example of the fluorescent traces obtained is shown in Figure 4b. The shape of the stopped flow transients obtained can be explained by the effective association rates (k_{on} multiplied by the concentration of substrate) of mFpp and GGpp being comparable, while the dissociation rate of the labeled compound is faster than that of the unlabeled one. A related case is dealt with in detail in ref *26*. The exact relationships between binding and dissociation rates of GGpp in this experiment are complex and can only be analyzed using numerical fitting. The global fitting procedure described in the Materials and Methods section was used to determine the following rate constants for GGpp: $k_{+1} = 0.28\ s^{-1}\ nM^{-1}$, $k_{-1} = 14\ s^{-1}$, $k_{+2} = 3.7\ s^{-1}$, and $k_{-2} = 6\ s^{-1}$. To be able to carry out the global fits, the fluorescent yields and rate constants obtained for mFpp (Figure 3c) were kept constant in the analysis (Figure 3d). Best fits were obtained when the binding of GGpp was modeled as consisting of two steps. On the basis of the obtained rate constants, we calculated a K_d value of 31 nM for yRabGGTase interaction with GGpp, which is in reasonable agreement with the previously determined K_d value of 14 nM.

Interaction of RabGGTase with Fpp. Prenyl transferases can associate with both GGpp and Fpp, albeit with different affinities. We used the strategy outlined above for studying the interaction of yRabGGTase with Fpp. Although the spectroscopic properties of mGpp are very similar to those of mFpp, FRET from tryptophans of the protein to the mant group was used due to the lower affinity of yRabGGTase for this isoprenoid. We titrated 100 nM yRabGGTase with increasing concentrations of phosphoisoprenoid. The data were corrected for directly exited fluorescence of the lipid and fitted as above resulting in a K_d value of 3 ± 0.2 μM for the yRabGGTase:mGpp interaction (Figure 4a). Kinetic constants for the interactions were also determined. Association reactions were monitored by rapidly mixing 50 nM yRabGGTase with increasing concentrations of mGpp. The traces could be fitted as double exponential with only the first phase being clearly concentration-dependent (data not shown). From the linear fit of the observed rate constants, we could determine the value of k_{+1} as $0.16\ s^{-1}\ nM^{-1}$ (Figure 4b). The dissociation rate could be estimated from the interception with the ordinate and was estimated to be ca. $200\ s^{-1}$. To determine the dissociation rate using a direct method, we rapidly mixed 50 nM yRabGGTase:mGpp complex with 2 μM GGpp. This resulted in a decrease of fluorescence as shown in Figure 4c. The data could be fitted with a double exponential function. From the fit of the data, we could obtain the values for k_{-1} and k_{-2} as 148 and 50 s^{-1}, respectively. On the basis of the obtained rate constants, we estimated a K_d value of 886 nM for yRabGGTase interaction with mGpp. The precise calculation of the K_d requires information about the k_{+2} rate. However, we assume that the second step is easily reversible due to the high k_{-2} and therefore does not significantly influence the overall equilibrium.

To determine the affinity of the RabGGTase toward Fpp, we performed a competition experiment. A mixture of 10 μM mGpp and RabGGTase was titrated with increasing concentrations of Fpp and monitored using the FRET signal. The curve obtained under these conditions was fitted numerically using the affinity for mGpp obtained from the transient kinetic experiments. This procedure yielded a K_d value of ca. 730 nM for yRabGGTase interaction with Fpp (Figure 4d).

Interaction of Yeast RabGGTase with its Protein Substrate. As mentioned in the Introduction, RabGGTase requires the assistance of the REP/Mrs6p molecule to carry out prenylation of Rab/Ypt proteins. To characterize this interaction, we made use of large fluorescence changes of a dansyl group attached to the C terminus of Rab proteins upon interaction with REP or RabGGTase (*18*). For our experiments, we chose the Ypt1p protein, which is essential for the first two steps of the yeast secretory pathway (*28*). We tested whether the fluorescent Ypt1p derivative could report on the interaction of RabGGTase with the Ypt1p:Mrs6p complex. When RabGGTase was added to a complex of dans Ypt1p and Mrs6p, a fluorescence increase of approximately 25% was observed (data not shown). There was no observable fluorescence change if RabGGTase was added to dansylated Ypt1p in the absence of Mrs6p, in agreement with the conclusion that only the Ypt1p:Mrs6p complex was recognized by RabGGTase (data not shown) (*22*). Under the conditions chosen, most of the Ypt1p is complexed to the Mrs6p, since the concentrations of the components are >10-fold higher than the K_d for Ypt1p:Mrs6p interaction (Constantinescu and Alexandrov, unpublished). We next titrated 300 nM dans_Ypt1p:Mrs6p with RabGGTase, and the obtained data were fitted using a quadratic equation to give

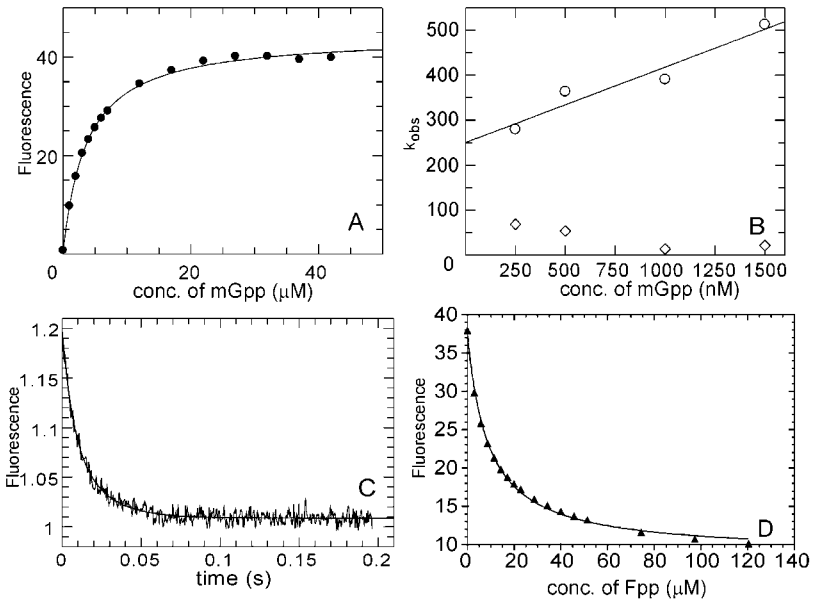

FIGURE 4: Fluorescence titration of RabGGTase (100 nM) vs increasing concentrations of mGpp. Fluorescence was exited with FRET from tryptophan at 286 nm, and data were collected at 440 nm. The experimental curve was corrected for background fluorescence and fitted resulting in a K_d value of 3 ± 0.2 μM (A). Secondary plot of data from the fluorescent energy transfer signal change seen on mixing of yRabGGTase (50 nM) with increasing concentrations of mGpp in the stopped flow apparatus. Open circles represent k_{1obs}, and open diamonds represent k_{2obs} values plotted against the concentration of yRabGGTase. The k_1 for yRabGGTase:GGpp obtained from the slope of the plot is 0.16 ± 0.3 s^{-1} nM^{-1} (B). The fit shown is to a double exponential equation with rate constants k_{-1} and k_{-2} for the displacement of yRabGGTase:mGpp: by GGpp of 148 ± 28 and 50 ± 6 s^{-1}, respectively (C). Competitive titration where a mixture of 10 μM mGpp and yRabGGTase was titrated against increasing concentrations of Fpp. The K_d determined form the fit for Fpp was 730 ± 90 nM (D).

a K_d value of 63 ± 7 nM and a 1:1:1 stoichiometry of the proteins (Figure 5a). If the titration experiment was repeated in the presence of excess of GGpp, the affinity of yRabGGTase for the Ypt1:Mrs6p complex was found be ca. 340 nM (data not shown). This difference in affinities can be explained by the interaction of the dansyl group of the Rab protein with the active site of RabGGTase. This interaction leads to an increase in affinity of the RabGGTase for the dansylated Rab:REP complex (*18*). Binding of GGpp to the RabGGTase competes with the dansyl group and weakens the interaction (Alexandrov, unpublished).

To determine the affinity of the unmodified Ypt1p:Mrs6p complex for yRabGGTase, we mixed 100 nM dans Ypt1p:Mrs6p complex with a 20-fold excess of wild-type Ypt1p:Mrs6p complex. The resulting mixture was titrated with yRabGGTase (Figure 5b). The data obtained were fitted using the program Scientist as described under Materials and Methods. Keeping the K_d for the fluorescent Rab7:REP-1 constant at the independently determined value of 63 nM, a K_d value of 329 ± 10 nM was obtained for the unmodified complex (Figure 5b).

Our earlier studies on mammalian RabGGTase demonstrated that the prenylated Rab:REP complex remains tightly associated with the transferase. This interaction is weakened by binding of a new phosphoisoprenoid to the ternary complex, enabling the release of the prenylated product (*10*). To test whether yeast RabGGTase utilizes a similar reaction mechanism, we prenylated the Ypt1p:Mrs6p complex in vitro using the recombinant yeast GST-RabGGTase fusion protein by an approach described earlier (*19*). In the following experiment, 2 μM prenylated Ypt1p:Mrs6p was mixed with 100 nM dans Ypt1p:Mrs6p complex. The mixture was titrated with increasing concentrations of yRabGGTase. In contrast to earlier observations on mammalian RabGGTase (*10*), the curve obtained was not sigmoidal, indicating that yRabGGTase bound to both proteins with comparable affinities (Figure 5c). The data obtained were fitted as described under Materials and Methods to give a K_d value of ca. 197 ± 5 nM for interaction of wild-type Ypt1pGG:Mrs6p with yRabGGTase (Figure 5c). This indicated that the affinity of Ypt1p:Mrs6p complex was only slightly affected by the presence of the conjugated geranylgeranyl moieties. To determine the effect of lipid substrate on product release, the titration described above was performed in the presence of 8 μM GGpp. Fitting of the observed binding isotherm using the approach outlined above led to a K_d value of 1.1 ± 0.01 μM for the interaction of Ypt1pGG:Mrs6p complex with RabGGTase in the presence of GGpp (Figure 5d). This result indicates only a moderate decrease of binding affinity in the presence of GGpp.

Interaction of yRabGGTase and Mrs6p. Analysis of interaction of mammalian RabGGTase with its protein substrate revealed that binding of GGpp to RabGGTase results in a nearly 2 orders of magnitude increase of its affinity for the Rab:REP complex (*12*). It appears that this affinity increase is largely due to the isoprenoid-modulated direct interaction of RabGGTase and REP. Indeed, binding of GGpp to RabGGTase decreased the K_d value for REP from >2 μM to 10 nM (*12*). Our initial attempts to detect interaction of yRabGGTase with Mrs6p in the presence or absence of GGpp using solid state precipitation or fluorescence spectroscopy were unsuccessful (data not shown). We suspected that the interaction might be too weak to be detected by these methods and chose to investigate the thermodynamic properties of yRabGGTase:Mrs6p interactions by means of isothermal titration calorimetry (ITC). ITC

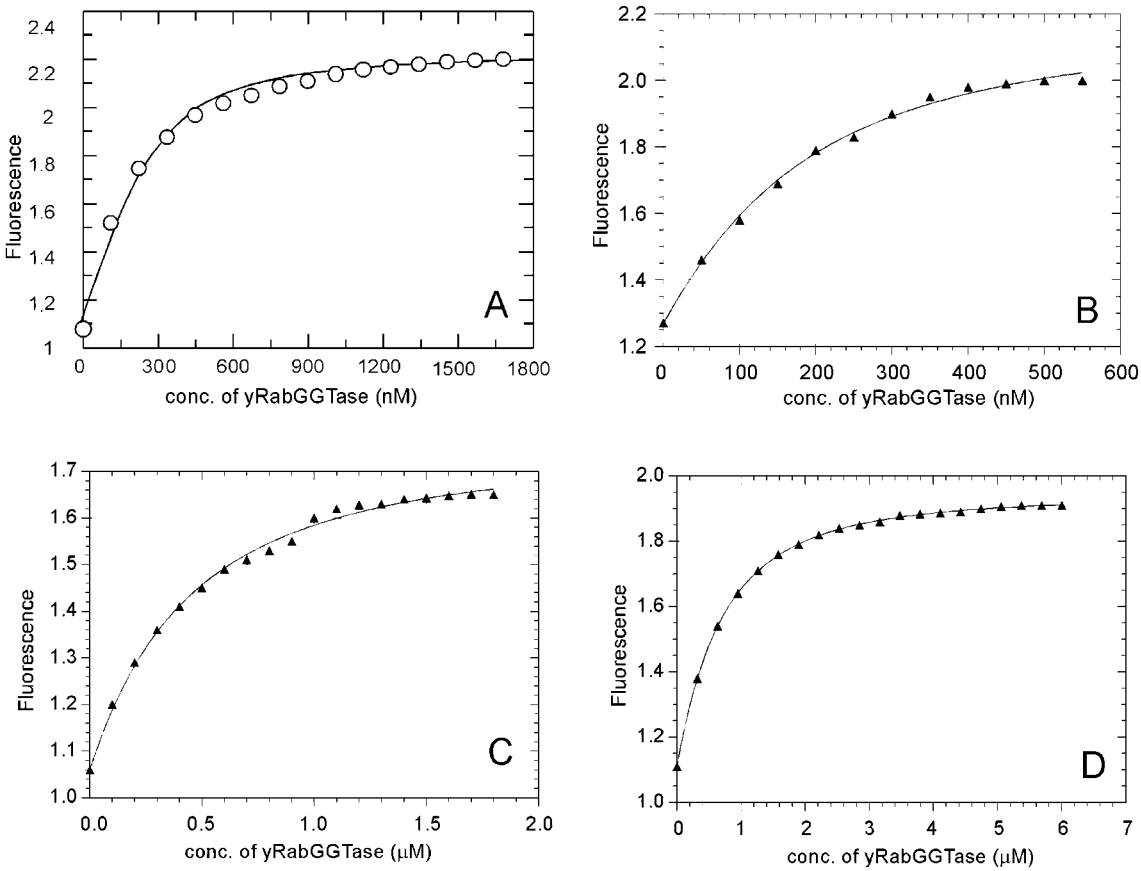

FIGURE 5: Titration of yRabGGTase to a nominal concentration of 300 nM dans_Ypt1p:Mrs6p using direct fluorescence as a signal for binding (excitation wavelength 338 nm, emission 490 nm). It can be inferred from the fit that 1 equiv of dans_Ypt1p:Mrs6p bound 1 equiv of yRabGGTase. The solid lines show the quadratic fit giving a value of 68 ± 12 nM for the K_d (A). Spectrofluorometric competition titration of dans_Ypt1p:Mrs6p (100nM) fluorescence by yRabGGTase in the presence of wild-type Ypt1p:Mrs6p complex (2 μM). Data were fitted using the program Scientist 2.0 and led to a K_d value of 329 ± 10 nM for the interaction of yRabGGTase with the unlabeled Ypt1p:Mrs6p complex (B). Competitive titration of dans_Ypt1p:Mrs6p (100 nM) mixed with prenylated Ypt1p:Mrs6p complex (2 μM). Data were fitted as above leading to a K_d value of 197 ± 5 nM (C). Competitive titration of dans_Ypt1p:Mrs6p (100 nM) mixed with prenylated Ypt1p:Mrs6p complex (2 μM) in the presence of 8 μM GGpp. The fit of the data yielded a K_d value of 1.0 ± 0.01 μM (D).

is well-suited for this study because it directly measures the enthalpy of association, H_0, and the affinity constant, K_a (*29*). Two sets of experiments were performed. In the first set, a 20 μM solution of Mrs6p was titrated stepwise with 200 μM solution yRabGGTase. A typical profile of such an experiment is presented in Figure 6a. The data could be fitted using the approach outlined in Materials and Methods to yield a K_a value of 2.6 ± 0.3 μM. This is in accord with previous estimations for interaction of mammalian RabGGTase and REP-1 (*12*). In the second set of experiments, both syringes were supplemented with 400 μM GGpp. The titration profile obtained under these conditions was noisier than in the previous experiment, probably due to the presence of high concentrations of GGpp (Figure 6b). Although the fit to the data was not very reliable, it could be concluded with certainty that the K_d value for the interaction was still in the micromolar range or higher, i.e., the affinity was not significantly increased.

Presence of LRR and Ig Domains Is Not Critical for Prenylation Reaction Mediated by RabGGTase. Sequence comparison of yeast and mammalian RabGGTase reveals that the yeast enzyme does not possess the Ig and LRR domains found in the mammalian transferase (Figure 1). These domains were proposed to be involved in interaction with the REP molecule (*4*). Having demonstrated that the phosphoisoprenoid-regulated alternative pathway of the catalytic complex assembly is not present in yRabGGTase, we wanted to establish whether the alternative pathway is essential for the prenylation reaction in the mammalian RabGGTase. To this end, we performed an in vitro prenylation reaction with combinations of both mammalian and yeast components of the prenylation machinery. Different combinations of mammalian RabGGTase, REP-1, Rab7, yRabGGTase, Mrs6p, and Ypt7p were incubated with [^{3}H]-GGpp and the amount of protein-bound radioactivity was measured. As can be seen in Figure 7, all combinations displayed incorporation of tritiated geranylgeranyl above background levels. The lowest incorporation was observed when the Mrs6p:Ypt7p complex was incubated with mammalian RabGGTase. When the Rab7:REP-1 complex was incubated with yRabGGTase, incorporation was efficient, although lower than in the case of the "all mammalian" enzyme. These results demonstrate that the presence of the Ig and LRR domains are not required for the catalytic activity of mammalian RabGGTase.

REP-1 Cannot Functionally Substitute MRS6 In Vivo. Having shown in vitro that mechanism of Rab/YPT prenylation is evolutionarily conserved, we wanted to address whether the components of prenylation machinery are interchangeable between mammals and yeast in vivo. To this

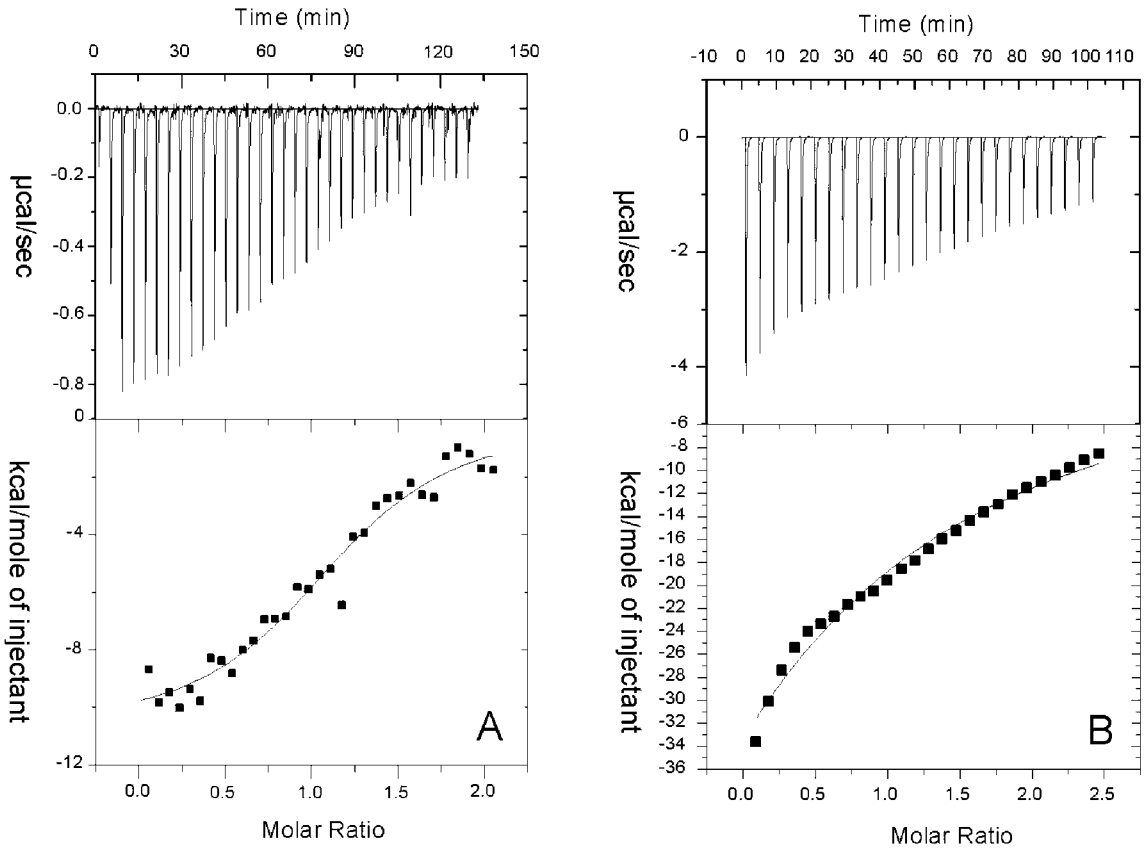

FIGURE 6: ITC titration of the RabGGTase with increasing concentrations of Mrs6p in the absence (A) and in the presence (B) of excess of GGpp. Fit of the data led to a K_d value of 2.6 ± 0.3 μM (A) and >5 μM (B).

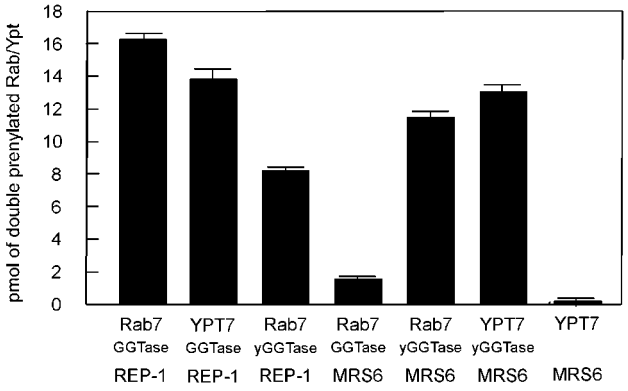

FIGURE 7: In vitro prenylation assay using [^{3}H]-labeled GGpp. Incorporation of [^{3}H]geranylgeranyl in Rab7 and Ypt1p catalyzed by mammalian and yRabGGTase. The reactions contained 100 pmol of [^{3}H]-labeled GGpp, 40 pmol of REP-1 or Mrs6p in complex with Rab7 or Ypt1p, and 3.4 pmol of mammalian or yeast RabGGTase.

end, we tested the ability of REP-1 to complement the deletion of *MRS6* gene in *S. cerevisiae*. A diploid yeast strain heterozygous at the *MRS6* locus (*MRS6*::*kanMX4*/+) was transformed with pYX212/REP-1 expression vector that contains cDNA of REP-1 under the control of TPI constitutive promoter. The expression of REP-1 in the transformed cells was confirmed by Western blotting (data not shown). The cells were sporulated and subjected to the tetrad analysis. As can be seen in Figure 8, the presence of the REP-1-expressing plasmid had no effect on the viability of spores as compared to the untransformed strain, indicating that REP-1 could not functionally substitute Mrs6p in vivo.

DISCUSSION

In this work, we have investigated to what extent the structural differences between mammalian and yeast RabGGTases affect their functional mechanism. We analyzed the interaction of RabGGTase with its isoprenoid and protein substrates using a combination of fluorescence spectroscopy, ITC, and in vitro prenylation assays.

Longer Isoprenoid Substrates Are Bound More Tightly. Using a cotitration approach, we determined the K_d of yRabGGTase for GGpp and Fpp to be 14 and 780 nM, respectively. Applying the stopped flow technique, we analyzed the binding kinetic of mFpp, mGpp, and GGpp interaction with yRabGGTase. The kinetics of the different isoprenoids demonstrate that all substrates tested have similar second order association rate constants. The difference in affinities is primarily due to variations in the dissociation rates. The tightest binding substrate, GGpp (K_d = 40 nM), has a dissociation rate constant (k_{-1}) of 14 s^{-1}, while mFpp (K_d = 364 nM) has a k_{-1} value of 162 s^{-1} and mGpp (K_d = 886) has a k_{-1} value of 148 s^{-1}. This finding is in accord with earlier findings on the mechanism of isoprenoid binding by RabGGTase. It is worth noting that both association and dissociation rates are much slower in yRabGGTase than in mammalian RabGGTase (*26*). The data also show that that the length of the isoprenoids has an influence on their affinity for yRabGGTase. This is in accord with earlier observations on the mammalian RabGGTase where the difference in affinity for GGpp and Fpp was found to be ca. 10-fold (*26*). However, both isoprenoids bind to yRabGGTase with much weaker affinity than to its mammalian counterpart. Therefore, unlike the mammalian enzyme, yRabGGTase might dis-

Scheme 2: Schematic Representation of Major Reaction Steps in Ypt1p Prenylation Reaction Catalyzed by yRabGGTase

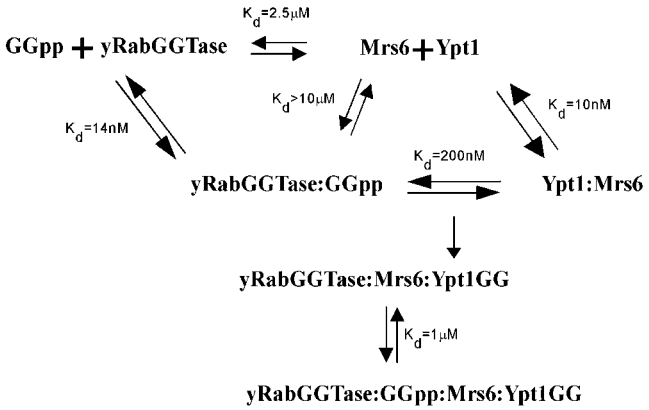

criminate between Fpp and GGpp in vivo solely on the basis of affinity. It is currently unknown how mammalian RabGGTase compensates for the lack of specificity in vitro (*26*), and the role of the alternative pathway in this process cannot be ruled out.

Interaction of yRabGGTase with Its Protein Substrate Complex. To analyze the interaction of Ypt1p:Mrs6p complex with yRabGGTase, we again employed a cotitration strategy using danyslated Ypt1p protein (*18*). We found that the affinity of yRabGGTase for its protein substrate was ca. 200 nM. This affinity is close to what has been observed for Rab7:REP-1 complex interaction with RabGGTase (120 nM) (*18*). However, unlike in the case of mammalian RabGGTase, where the prenylated complex binds to RabGGTase with an affinity of ca. 2 nM, the prenylated Ypt1p:Mrs6p complex interacts with yRabGGTase with a K_d of ca. 200 nM, indicating that both substrate and product bind to the enzyme with similar affinities. The presence of GGpp results in a decrease of affinity to ca. 1 μM indicating that as in the case of mammalian RabGGTase lipid substrate binding induces product release (Scheme 2). However, both in the presence and in the absence of GGpp, the affinities of yRabGGTase for its product are still approximately 50 times weaker than in the case of the mammalian enzyme. The implications of this finding are unclear at present and could potentially reflect differences in organization and regulation of the Ypt/Rab prenylation machinery in yeast and mammalian cells.

Interaction of yRabGGTase and Mrs6p. We recently demonstrated that REP-1 and mammalian RabGGTase can interact directly with high affinity in the presence of phosphoisoprenoids (*12*). It has been proposed that the LRR domain and the Ig-like domain could be responsible for making contact to the REP molecule (*4*). Both of these regions are missing in yRabGGTase, as concluded on the basis of the sequence analysis (Figure 1). We tested the direct interaction of yRabGGTase and Mrs6p using ITC. It transpired from these experiments that in the absence of the GGpp, the affinity was approximately 2.6 μM. This is close to the affinity estimated for the RabGGTase:REP-1 interaction and is in agreement with earlier results (*12, 30*). However, the presence of GGpp did not result in tighter binding of yRabGGTase to Mrs6p. Although the final conclusion can be reached only upon full kinetic characterization of the prenylation reaction, this finding suggests that yRabGGTase follows only the classical pathway of catalytic complex assembly (Scheme 2). In this pathway, the reaction is initiated by Rab:REP complex formation and is followed by addition of RabGGTase:GGpp complex. From this perspective, it appears that the alternative pathway involving formation of RabGGTase:GGpp:REP-1 complex formation occurs only in vertebrate cells. It seems likely that either the LRR or the Ig-like domains of mammalian transferase are involved in the lipid-regulated RabGGTase:REP interaction. To address the possible role of these domains in prenylation catalysis, we performed in vitro prenylation reactions using different combinations of subunits of mammalian and yeast RabGGTase. This experiment demonstrated that the Rab7:REP-1 complex could be prenylated by yRabGGTase, albeit with lower efficiency than in the all mammalian system. These data indicate that the prenylation machinery is highly conserved from yeast to mammals. The results also demonstrate that the presence of LRR or Ig-like domains is not essential for enzymatic activity of RabGGTase. We propose that the basic function of RabGGTase has been retained throughout evolution and new functional domains have been integrated to perform additional and as yet unidentified functions. The role of the alternative pathway in Rab prenylation thus remains unknown and will require further studies.

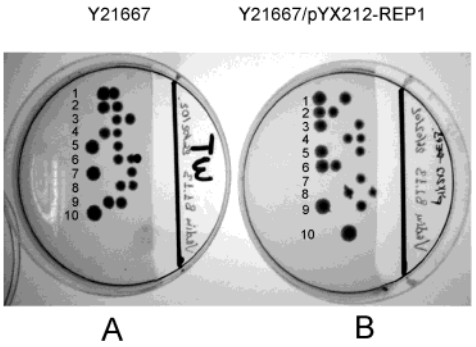

FIGURE 8: Spore viability for Y21667 (A) and Y21667/pYX212/REP-1 (B) strains tested by tetrad analysis. Yeast cells were sporulated, and the dissected tetrads were incubated on YPD plates at 30 °C for 5 days. Row 6 in panel A has a plating defect.

Finally, we analyzed the ability of REP-1 to complement the *MRS6* gene deletion in yeast *S. cerevisiae*. Our results demonstrate that the ability of REP-1 to support prenylation of Rab/YPT proteins by yRabGGTase is not alone sufficient for its functional substitution of Mrs6p in vivo. It is probable that REP-1 fails to properly deliver prenylated YPT protein to their target membranes. This finding is not all that surprising taking in consideration the difference in the organization of yeast and mammalian machineries of vesicular transport.

ACKNOWLEDGMENT

Thanks are due to A. T. Constantinescu for critically reading the manuscript. We are grateful to D. Poulter and S. Ferro-Novick for providing the expression vectors for Bet-2, Bet-4, and Mrs6p. H. Walldman is gratefully acknowledged for the gift of mFpp and mGpp. Thanks are also due to D. Gallwitz for providing expression constructs for Ypt7p and Ypt1p. We acknowledge S. Uttich for invaluable technical assistance.

REFERENCES

1. Gelb, M. H., Scholten, J. D., and Sebolt-Leopold, J. S. (1998) *Curr. Opin. Chem. Biol. 2*, 40−48.
2. Rowinsky, E. K., Windle, J. J., and Von Hoff, D. D. (1999) *J. Clin. Oncol. 17*, 3631−3652.
3. Casey, P. J., and Seabra, M. C. (1996) *J. Biol. Chem. 271*, 5289−5292.
4. Zhang, H., Seabra, C. M., and Deisenhofer, J. (2000) Crystal structure of Rabgeranylgeranyltransferase at 2.0A resolution. *Structure 8*, 241−251.
5. Jiang, Y., and Ferro-Novick, S. (1994) *Proc. Natl. Acad. Sci. U.S.A. 91*, 4377−4381.
6. Andres, D. A., Seabra, M. C., Brown, M. S., Armstrong, S. A., Smeland, T. E., Cremers, F. P., and Goldstein, J. L. (1993) *Cell 73*, 1091−1099.
7. Alexandrov, K., Horiuchi, H., Steele-Mortimer, O., Seabra, M. C., and Zerial, M. (1994) *EMBO J. 13*, 5262−5273.
8. Alory, C., and Balch, W. E. (2001) *Traffic 2*, 532−543.
9. Pereira-Leal, J. B., Hume, A. N., and Seabra, M. C. (2001) *FEBS Lett. 498*, 197−200.
10. Thoma, N. H., Iakovenko, A., Kalinin, A., Waldmann, H., Goody, R. S., and Alexandrov, K. (2001) *Biochemistry 40*, 268−274.
11. Wilson, A. L., Erdman, R. A., and Maltese, W. A. (1996) *J. Biol. Chem. 271*, 10932−10940.
12. Thoma, N. H., Iakovenko, A., Goody, R. S., and Alexandrov, K. (2002) *J. Biol. Chem.* (in press).
13. Stirtan, W. G., and Poulter, C. D. (1997) *Biochemistry 36*, 4552−4557.
14. Yokoyama, K., Zimmerman, K., Scholten, J., and Gelb, M. H. (1997) *J. Biol. Chem. 272*, 3944−3952.
15. Mathis, J. R., and Poulter, C. D. (1997) *Biochemistry 36*, 6367−6376.
16. Furfine, E. S., Leban, J. J., Landavazo, A., Moomaw, J. F., and Casey, P. J. (1995) *Biochemistry 34*, 6857−6862.
17. Owen, D. J., Alexandrov, K., Rostkova, E., Scheidig, A. J., Goody, R. S., and Waldmann, H. (1999) *Angew. Chem. Int. Ed. 38*, 509−512.
18. Alexandrov, K., Simon, I., Yurchenko, V., Iakovenko, A., Rostkova, E., Scheidig, J., and Goody, R. S. (1999) *Eur. J. Biochem. 265*, 160−170.
19. Kalinin, A., Thoma, N. H., Iakovenko, A., Heinemann, I., Rostkova, E., Constantinescu, A. T., and Alexandrov, K. (2001) *Prot. Exp. Purif. 22*, 84−91.
20. Vollmer, P., Will, E., Scheglmann, D., Strom, M., and Gallwitz, D. (1999) *Eur. J. Biochem. 260*, 284−290.
21. Wagner, P., Hengst, L., and Gallwitz, D. (1992) *Methods Enzymol. 219*, 369−387.
22. Witter, D. J., and Poulter, C. D. (1996) *Biochemistry 35*, 10454−10463.
23. Thoma, N. H., Niculae, A., Goody, R. S., and Alexandrov, K. (2002) *J. Biol. Chem.* (in press).
24. Armstrong, S. A., Brown, M. S., Goldstein, J. L., and Seabra, M. C. (1995) *Methods Enzymol. 257*, 30−41.
25. Rudolph, M. G., Linnemann, T., Grunewald, P., Wittinghofer, A., Vetter, I. R., and Herrmann, C. (2001) *J. Biol. Chem. 276*, 23914−23921.
26. Thoma, N. H., Iakovenko, A., Owen, D., Scheidig, A. S., Waldmann, H., Goody, R. S., and Alexandrov, K. (2000) *Biochemistry 39*, 12043−12052.
27. Agatep, R., Kirkpatrick, R. D., Parchaliuk, D. L., Woods, R. A., and Gietz, R. D. Transformation of *Saccharomyces cerevisiae* by the lithium acetate/single-stranded carrier DNA/poly(ethylene glycol) (LiAc/ss-DNA/PEG) protocol. (http://tto.trends.com). 1998.
28. Lazar, T., Gotte, M., and Gallwitz, D. (1997) *Trends. Biochem. Sci. 22*, 468−472.
29. Wiseman, T., Williston, S., Brandts, J. F., and Lin, L. N. (1989) *Anal. Biochem. 179*, 131−137.
30. Alory, C., and Balch, W. E. (2000) *J. Cell Biol. 150*, 89−103.

BI016067W